

Fluid migration paths in the marine strata of typical structures in the western Hubei–eastern Chongqing area, China

Xu Guosheng¹, Liang Jiaju^{1*}, Gong Deyu², Wang Guozhi¹, Yuan Haifeng¹, Cao Junxing¹ and Zhang Chengfu³

¹ State Key Laboratory of Oil and Gas Reservoir Geology and Exploitation (Chengdu University of Technology), Sichuan 610059, China

² Research Institute of Petroleum Exploration and Development, PetroChina, Beijing 100083, China

³ SINOPEC Zhongyuan Oilfield Company, Puyang, Henan 457000, China

© China University of Petroleum (Beijing) and Springer-Verlag Berlin Heidelberg 2013

Abstract: The western Hubei–eastern Chongqing area is an important prospective zone for oil and gas exploration in the central Yangtze area. Three representative structures, the Xinchang structure, Longjuba gas-bearing structure and the Jiannan gas field, were selected to analyze biomarker parameters in marine strata and to examine various types of natural gas and hydrocarbon sources. Fluid inclusions; carbon, oxygen, and strontium isotopic characteristics; organic geochemical analysis and simulation of hydrocarbon generation and expulsion history of source rocks were used for tracing fluid migration paths in marine strata of the study area. The Carboniferous–Triassic reservoirs in three typical structures all experienced at least two stages of fluid accumulation. All marine strata above the early Permian were shown to have fluids originating in the Permian rocks, which differed from the late stage fluids. The fluids accumulated in the late Permian reservoirs of the Xinchang structure were Cambrian fluids, while those in the late Carboniferous reservoirs were sourced from a combination of Silurian and Cambrian fluids. A long-distance and large-scale cross-formational flow of fluids destroyed the preservation conditions of earlier accumulated hydrocarbons. A short-distance cross-formational accumulation of Silurian fluids was shown in the late Permian reservoirs of the Longjuba structure with favorable hydrocarbon preservation conditions. The fluid accumulation in the Carboniferous reservoirs of the Jiannan structure mainly originated from neighboring Silurian strata with a small amount from the Cambrian strata. As a result, the Jiannan structure was determined to have the best preservation conditions of the three. Comparative analysis of fluid migration paths in the three structures revealed that the zone with a weaker late tectonism and no superimposition and modification of the Upper and Lower Paleozoic fluids or the Upper Paleozoic zone with the fluid charging from the Lower Paleozoic in the western Hubei–eastern Chongqing area are important target areas for future exploration.

Key words: Western Hubei–eastern Chongqing area, marine strata, geochemical tracer, fluid migration path

1 Introduction

The marine carbonate areas of the superimposed basins in the south of China have become important targets for exploration for oil and gas in China. However, as they have a deep burial depth and have experienced multiple cycles of structural movements and intense post-reconstructions, the geological conditions of these areas are especially complicated. The most influential movements are the

Caledonian, Dongwu, Indo-Sinian, Yanshan and Himalayan movements. The multi-phase tectonic activities have to a certain degree reformed and damaged the early excellent preservation condition. It is safe to say that the preservation condition has become a key factor restricting the exploration for oil and gas in these marine carbonate areas in the south of China. Scholars have studied the preservation condition from such perspectives as caprock physical properties, hydrodynamic environment, sealing ability of faults and tectonic movements. It is not possible for us to evaluate the static preservation condition of the complicated areas that have gone through multi-phase tectonic activities from only the perspective of general parameters of caprock physical

*Corresponding author. email: liangjiaju830@qq.com

Received June 8, 2011

properties. We have found a new way to evaluate the preservation condition of the marine oil and gas from the perspective of paleofluid geochemistry. A dynamic evaluation can be conducted for the preservation condition of the areas that have experienced multi-phase tectonic activities. The following three typical structures that differ significantly in exploration effectiveness, Xinchang, Longjuba, and Jiannan, were chosen as cases to analyze oil and gas sources in the marine strata of western Hubei–eastern Chongqing area and to trace fluid migration paths. This is expected to shed light on the formation, evolution, destruction and modification of different structures and to provide a scientific basis for further exploration for oil and gas in this area.

2 Geological setting

The western Hubei–eastern Chongqing area, which

is a part of the central Yangtze area (Xu and Lin, 2001; Liu et al, 2007), is geographically located in the western Hubei Province and eastern Chongqing City. This area is geotectonically classified as a depression belt of the Dabashan front in the eastern margin of the Sichuan Basin, covering Wanxian, Shizhu, and Lichuan synclinoriums, Fangdoushan and Qiyueshan anticlinoriums, and other tectonic units (Fig. 1). The study region has an area of 21,200 km², and secondary structures are developed which include the Yupize, Liangqiao, Cizhuya, Gaofengchang, Macaoba, Dachiganjing, Huangjintai, Yanjing, Chayuanping, Xinchang, Jiannan, and Longjuba structures. Numerous gas fields including Jiannan, Gaofengchang, and Dachiganjing, and gas-bearing structures including Yupize, Yangduxi, Cizhuya, Yanjing, and Longjuba, have already been discovered.

Marine basins were developed in the central Yangtze

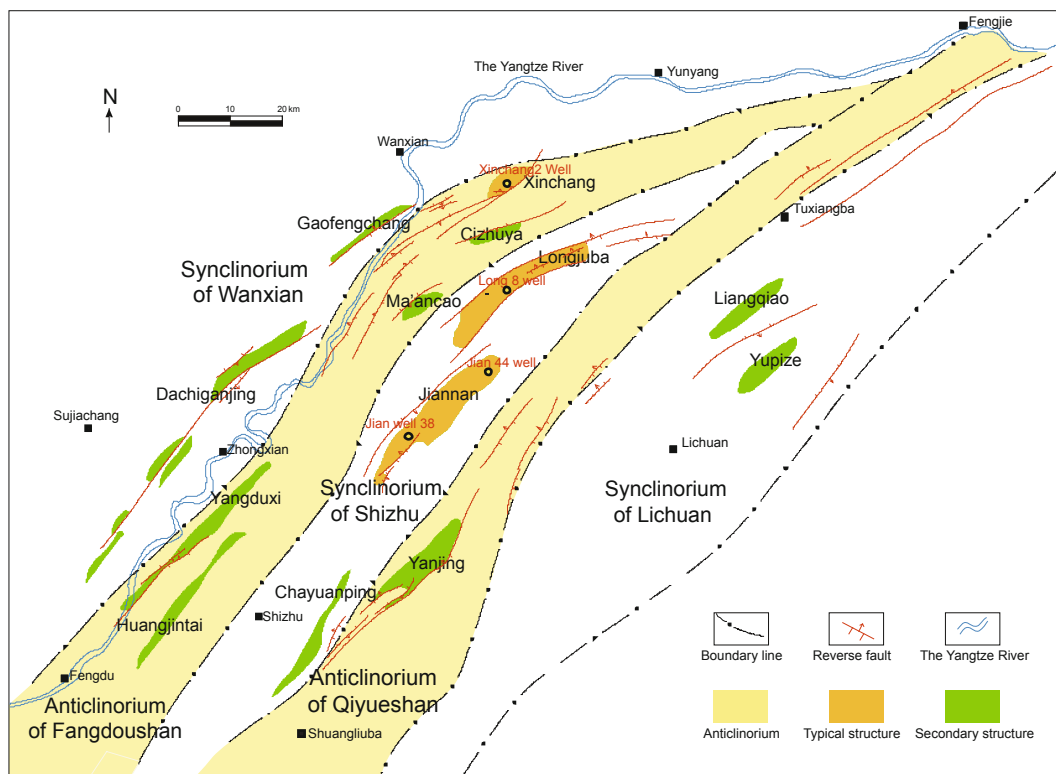


Fig. 1 Classification of tectonic units in the western Hubei–eastern Chongqing area and location diagram of typical structures

area from the early Sinian period of the Late Proterozoic to the late Early Triassic of the Mesozoic era. The study area experienced Caledonian and Indo-Sinian closure and orogeny in the South China and Paleo-Qinling oceans, where two stages of mass marine regression occurred, and marine strata were developed mainly as deep-water basin and shallow platform facies (Fig. 2). Multiple sets of source-reservoir-seal assemblages were developed vertically. Two sets of large source-reservoir-seal assemblages (i.e., upper and lower assemblages) were divided by extremely thick Silurian shale as the boundary, constituting the two major exploration regions in this study area (Wu, 1997; Yang et al,

1999; Fu et al, 1999; Liu et al, 1999; Xu and Lin, 2001; Chen et al, 2007). The area west of the Qiyueshan anticlinorium to the Fangdoushan anticlinorium and the Shizhu synclinorium is characterized by favorable preservation conditions with a high degree of trap identification. In addition, the area is situated in a beneficial paleo-tectonic position for hydrocarbon migration and accumulation, which makes it a favorable exploration zone (Guo et al, 2008). The Qiyueshan anticlinorium and its eastern part as well as the Lichuan synclinorium are comparatively prospective zones (Dai et al, 2001). In the Longjuba-Jiannan structure echeloned in the central Shizhu synclinorium, a hydrocarbon accumulation

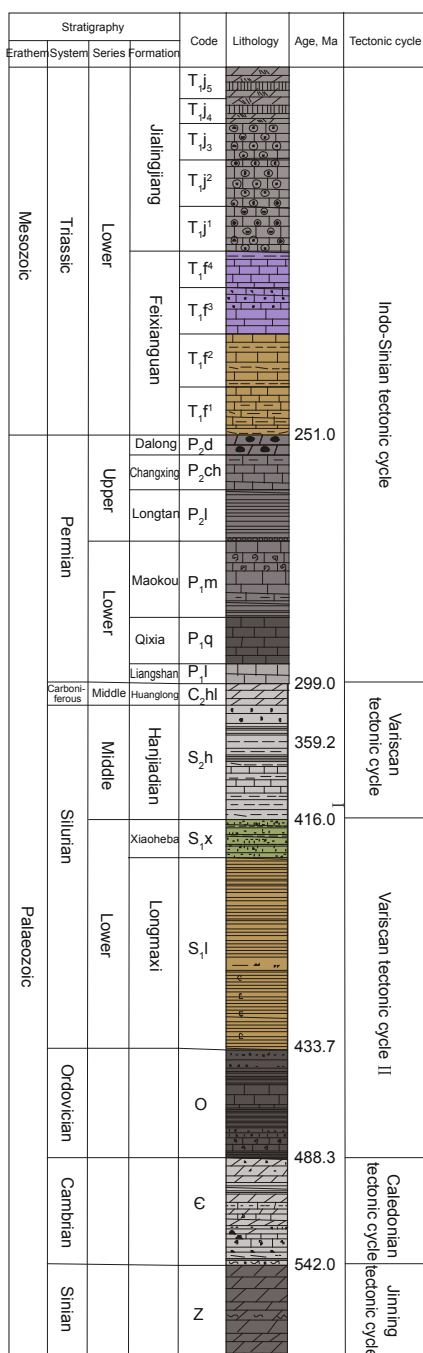


Fig. 2 Synthetic column map of Z-T₁ in the western Hubei-eastern Chongqing area showing tectonic cycles

belt was formed with Jiannan as the center. The Jiannan gas field was discovered in the central syncline, proving that the Longjuba-Jiannan structure had favorable preservation conditions for gas reservoirs in addition to a tectonic setting for hydrocarbon accumulation (Chen, 2003; Gao, 2004).

3 Sample analysis

As is widely accepted, kerogen in source rocks is cracked into petroleum and natural gas under certain conditions, and hydrocarbon in source rocks has a genetic relationship with bitumen in addition to oil and gas in the rock reservoirs. Thus, similarities exist in the chemical

compositions of hydrocarbons from the same source rocks, while large differences are evident in those from different source rocks. Such similarities serve as a basis for oil-source correlation. Currently, gas chromatography and mass spectrometry (GC-MS) provide widely used biomarkers for oil-source correlation (Al-Meshari et al, 2009). Hydrocarbons are altered during biodegradation processes (Rowe and Muehlenbachs, 1999; Masterson, 2001) and groundwater scouring, resulting in incorrect oil-source correlation. However, the influences of external secondary factors are effectively reduced in the correlation processes through the use of such techniques as biomarkers and comprehensive comparison of various parameters. Although isotopes are the most important indicators in oil-gas comparisons (Hao et al, 2000), fractionation will occur in isotopes during hydrocarbon migration (Galimov et al, 1973; Karlsen et al, 1993; Boreham et al, 1998), which creates difficulties in gas-source correlation.

An model to estimate organic maturity on the basis of vitrinite reflectance was first completed by the time-temperature index (TTI) method (Waples, 1980) and this was then replaced by a model that calculates vitrinite reflectivity (R_o) more efficiently, known as the Easy% R_o dynamic model (Sweeney and Burnham, 1990). A thermal-related biomarker ratio was proposed by Mackenzie et al (Mackenzie et al, 1981; 1984; Mackenzie and Mckenzie, 1983) for basin modeling, so that the paleotemperature could be calculated more accurately (Welte and Yalcin, 1988; Ungerer, 1990). However, the Easy% R_o chemical kinetic model later proposed by Sweeney and Burnham (1990) is the most commonly used model in current studies on paleotemperature. On the basis of vitrinite reflectance measured from drilling cores, a better Easy% R_o dynamic simulation method with a broader application scope was used in this study to reconstruct the thermal history of source rocks and the evolutionary history of hydrocarbon generation. The previous R_o value was 0.3%-4.5%.

A secondary hydrocarbon migration and reservoir charge principle was described by England et al (1987; 1995), Rückheim and England (1989) and England and Mackenzie (1989), in which the component, phases, temperature, and other information on inclusions were used to calibrate the history of hydrocarbon charge and time of hydrocarbon accumulation. In addition, fluid inclusion stratigraphy was applied to fluid source and migration pathway research by some scholars (Barclay et al, 2000). The inclusion homogenization temperature discussed herein generally refers to that of hydrocarbon-bearing saline inclusion, rather than that of hydrocarbon inclusions. The homogenization temperature of hydrocarbon inclusions is often lower than that of saline inclusions of the same period (Lu and Guo, 2000). Inclusions are able to reflect the essential characteristics of ore-forming fluids and provide a series of original data on such mineral formation parameters as temperature, elemental composition, and salinity. A fluid geochemical tracer was combined with the inclusion test and analysis methods in this paper to study fluid migration path and charge durations.

We then determined biomarkers and stable carbon isotopes of natural gas, inclusions, carbon, oxygen, and strontium in

veins and surrounding rocks in addition to other geochemical analysis data and their sources.

Five new samples of potential source rocks and five samples of residual organic material in reservoirs were obtained from well Xinchang 2 in the western Hubei–eastern Chongqing area. A gas chromatograph (HP 6890; Hewlett Packard) and gas chromatograph-mass spectrometer (GC-MS UMSP-50) were used to measure total-hydrocarbon gas-chromatography, biomarkers, and vitrinite reflectance was measured with a microphotometer (Tables 1-3). Due to the high maturity of residual organic matter in the study area, the organic extract was too limited to permit the analysis of group components and their isotopes.

The analysis data of 17 natural gas samples in 16 wells were used in this study (Table 4 and Table 5), including one Permian natural gas sample from the well Long 8 in the Longjuba structure. Because the Permian natural gas in this

well is of high maturity, only methane and small amounts of ethane and propane were detected; thus, light hydrocarbon analysis could not be performed. As a result, the gas isotopic mass spectrometer MAT 252 was used to determine stable carbon isotopes of natural gas.

The collected samples of calcite and gypsum veins that filled fractures in reservoir rocks were tested by the Guiyang Institute of Geochemistry, Chinese Academy of Sciences. It was determined that hydrocarbon gases were contained in fluid inclusions. However, few hydrocarbon-bearing inclusions were detected. Thus, Molecular Composition of Oil Inclusion (MCI™) analysis could not be performed. Instead, laser Raman quantitative analysis was used on inclusion components. In addition, carbon, oxygen, and strontium isotopic values were obtained with the UK VG354 isotope mass spectrometer (TIMS) by the Isotope Mass Laboratory of Modern Analysis Center, Nanjing University (Table 6).

Table 1 Saturated hydrocarbon chromatography parameters of marine strata samples from well Xinchang 2

Sample No.	Depth, m	Horizon	Lithologic description	$\frac{C_{21}+C_{22}}{C_{28}+C_{29}}$	$\frac{\sum C_{21}}{\sum C_{22}}$	Pr/nC ₁₇	Ph/nC ₁₈	Pr/Ph
XC2-1	2824.42	T ₁ f ³	Dark gray limestone, potential source rocks	1.33	0.95	0.64	0.86	0.53
XC2-2	2828.22	T ₁ f ³	Black limestone, potential source rocks	/	3.16	1.05	1.42	0.55
XC2-11	2848.22	T ₁ f ³	Dark gray limestone, organic matter filled along suture zones	4.90	2.49	0.29	0.75	0.48
XC2-12	2853.83	T ₁ f ³	Gray-dark gray limestone, organic matter filled along suture zones	3.21	2.01	0.63	1.06	0.50
XC2-13	2862.90	T ₁ f ³	Light gray limestone, black organic matter filled along suture zones	12.75	1.99	0.75	0.96	0.60
XC2-14s	3338.35	P ₂ c ²	Black limestone, potential source rocks	1.82	1.34	0.43	0.74	0.51
XC2-20	3376.04	P ₂ c ²	Dark gray limestone, filled with massive organic matter	4.00	1.37	1.50	1.82	0.23
XC2-23s	4607.54	P ₁ q	Black coal rock, potential source rocks	/	2.22	0.83	1.10	0.59
XC2-22s	4608.54	P ₁ q	Black coal rock, potential source rocks	10.00	1.56	1.11	1.25	0.40
XC2-25	4623.04	C ₂ c	Gray dolomite, bitumen along suture zones and filled in factures	0.53	0.67	0.70	1.03	0.61

Table 2 Terpane and sterane biomarker parameters of marine strata samples from the well Xinchang 2

Sample No.	Horizon	Ts/Tm	$\frac{C_{29}Ts}{(C_{29}Ts+C_{29})}$	$\frac{C_{32}22S}{(22S+22R)}$	Gamma ₃₀ / hopane	Tricyclic-terpane / C ₃₀ hopane	$\frac{C_{29}aaa(20S)}{(20S+20R)}$	$\frac{C_{21}+C_{22}\text{-pregnane}}{C_{29}aaa(20R)}$	Diasterane / regular sterane
XC2-1	T ₁ f ³	0.69	0.21	0.59	0.26	1.06	0.38	0.44	0.14
XC2-2	T ₁ f ³	0.95	0.29	0.62	0.17	3.67	0.30	2.61	0.22
XC2-11	T ₁ f ³	0.56	0.25	0.59	0.26	0.49	0.41	0.23	0.07
XC2-12	T ₁ f ³	0.73	0.14	0.59	0.26	2.02	0.36	1.15	0.14
XC2-13	T ₁ f ³	1.61	0.18	0.62	0.34	0.58	0.35	1.14	0.26
XC2-14s	P ₂ c ²	0.50	0.09	0.59	0.29	0.26	0.46	0.09	0.06
XC2-20	P ₂ c ²	0.93	0.28	0.57	0.19	1.71	0.34	1.03	0.20
XC2-23s	P ₁ q	1.07	0.21	0.60	0.23	2.50	0.31	3.15	0.23
XC2-22s	P ₁ q	0.90	0.18	0.60	0.19	3.33	0.29	2.62	0.28
XC2-25	C ₂ c	0.98	0.18	0.60	0.29	1.26	0.37	0.58	0.41

Table 3 Aromatic characteristic parameters of samples from well Xinchang 2

Sample No.	Horizon	Relative content, %						Relative content, %			
		Phenanthrene	Chrysene	Dibenzothiophene, dibenzofuran, and fluorene	F/MF	F+MF+OF/DMF+DOF+SF	F/DMF	SF/P	Dibenzothiophene	Fluorene	Dibenzofuran
XC2-1	T ₁ f ³	94.34	/	5.66	0.978	0.244	/	0.047	78.50	/	21.50
XC2-2	T ₁ f ³	87.52	/	12.48	1.050	0.624	0.279	0.033	23.00	67.38	9.62
XC2-11	T ₁ f ³	93.90	/	6.10	3.222	0.993	0.547	0.003	5.38	80.52	14.10
XC2-12	T ₁ f ³	99.45	/	0.55	2.388	0.332	0.021	/	/	100.00	/
XC2-13	T ₁ f ³	84.16	/	15.84	1.162	2.225	/	0.032	16.94	67.56	15.50
XC2-14s	P ₂ c ²	93.46	/	6.54	2.851	0.751	0.368	0.006	8.23	84.58	7.19
XC2-20	P ₂ c ²	89.86	/	10.14	1.842	4.408	1.345	0.014	12.80	75.29	11.91
XC2-23s	P ₁ q	77.81	/	22.19	1.397	1.845	0.603	0.029	10.15	67.13	22.72
XC2-22s	P ₁ q	80.63	/	19.37	1.310	2.250	0.544	0.030	12.57	65.53	21.91
XC2-25	C ₂ c	89.57	/	10.43	0.894	0.716	0.110	0.031	26.93	47.67	25.40

Table 4 Conventional components of natural gas in C₂-T_{1j}¹ formations in the Jiannan-Longjuba structure and characteristics of carbon isotopes in well Long 8, Jiannan gas field, and adjacent areas. The data for the Jiannan structure is in accordance with that reported by Ma (2004)

Well No.	Formation	Depth, m	C ₁ , %	C ₂ , %	C ₃ , %	N ₂ , %	CO ₂ , %	H ₂ S, %	C ₁ /C ₁ -C ₅ , %
Long 8	P ₁ m		98.35	0.14	/	0.28	1.2	/	99.85
Jian 32	T _{1j} ¹	2494.05-2531	94.70	0.17	—	1.67	3.07	0.40	99.82
Jian 3	T ₁ f ³	2709-2762	96.04	0.20	—	0.31	2.93	0.52	99.79
Jian 10	T ₁ f ³	2927-2941	96.52	0.12	—	1.15	1.94	0.27	99.88
Jian 45	T ₁ f ³	3061-3089	94.93	0.21	—	1.87	2.81	0.18	99.78
Jian 15	T ₁ f ³	3110-3161.1	96.55	0.12	—	1.51	1.72	0.105	99.88
Jian 41	T ₁ f ³	3343.6-3402	92.00	0.14	—	0.84	4.51	2.48	99.85
Jian 47	T ₁ f ³	3614.4-3642.6	95.93	0.09	—	1.72	1.98	0.28	99.91
Jian 16	P ₂ c ²	3109.9-3229.6	86.73	0.17	—	1.19	8.56	3.36	99.80
Jian 40	P ₂ c ²	3329.6-3348.4	87.04	0.07	—	0.77	8.87	3.24	99.92
Jian 43	P ₂ c ²	3456-3483	92.05	0.19	—	0.26	5.70	1.80	99.72
Jian 44	P ₂ c ²	3738.11-3760.18	88.37	0.06	—	1.30	7.39	2.88	99.93
Jian 13	C ₂	3728.59-3748.15	94.31	1.22	0.24	3.39	0.68	0.162	98.72
Jian 37	C ₂	3836.4-3860.0	94.71	1.24	0.15	3.24	0.66	0	98.70
Jian 28	C ₂	3943-3950	94.57	1.23	0.13	3.51	0.56	0	98.72

Table 5 Analysis results of the carbon isotopes of the natural gas in the Longjuba structure and Jiannan gas field. The data for the Longjuba structure is in accordance with that of the Exploration and Development Research Institute of Jiangnan Oilfield

Structure location	Well No.	Formation	Depth, m	δ ¹³ C ₁ , ‰	δ ¹³ C ₂ , ‰	δ ¹³ C ₂ -δ ¹³ C ₁ , ‰
Longjuba	Long 8	P ₁ m		-29.9	-32.7	-2.8
The northern high point	Jian 31	T _{1j} ¹	2777.5-2856	-32.2	-37.8	-5.6
	Jian 31	T _{1j} ¹	2777.5-2856	-32.4	-36.4	-4.0
The southern high point	Jian 35	T ₁ f ³	3066.4-3114	-32.1	-38.4	-6.3
	Jian 27 Ceping1	T ₁ f ³	3680.78-4506.33	-31.0	-38.0	-7.0
	Jian 61	T ₁ f ³		-33.1	-41.4	-8.3
The northern high point	Jian 10	T ₁ f ³	2927-2941	-32.1	-37.4	-5.3
	Jian 10	T ₁ f ³	2927-2941	-31.4	-33.3	-1.9
	Jian 51	T ₁ f ³		-30.8	-28.5	2.3
Southern high point	Jian 43	P ₂ ch	3456-3483	-32.0	-38.9	-6.9
	Jian 43	P ₂ ch	3456-3483	-32.2	-37.2	-5.0
Northern high point	Jian 16	P ₂ ch	3109.9-3229.6	-31.7	-33.6	-1.9
	Jian 44 Yuan1	P ₂ ch	3145.94-3600	-33.5	-35.6	-2.1
Northern high point	Jian 34	C	3770-3784	-37.2	-41.4	-4.2
	Jian 28	C	3941-3950	-35.2	-40.0	-4.8
	Jian 28	C	3943-3950	-37.9	-41.4	-3.5

Table 6 Isotopic geochemical analysis results of different rocks and minerals in wells Xinchang 2, Long 8 and Jian 38

Well	Sample No.	Lithology	Well depth, m	Horizon	$\delta^{13}\text{C}$ (PDB), ‰	$\delta^{18}\text{O}$ (PDB), ‰	$^{87}\text{Sr}/^{86}\text{Sr}$
Xinchang 2	Xc2-15V	Grayish-white megacryst gypsum	3340.5		–	–	0.71
	Xc2-17V	Calcite veins	3370	P ₂ ch ²	4.708	-5.647	0.7075
	Xc2-17C	Dark grey micrite			4.632	-4.43	0.7071
	Xc2-21V	Grayish-white fine-medium grained calcite vein patch	3375.64		4.946	-6.98	0.7074
	Xc2-21C	Grey micrite		4.742	-4.19	0.707	
Long 8	Bao 10V	Grayish-white fine-medium grained calcite veins	4314.67	P ₂ ch ²	3.747	-6.263	0.7071
	Bao 10C	Grey micrite			4.086	-6.081	–
	Bao 19V	Grayish-white fine-medium grained calcite veins	4557.84	P ₁ m ³	4.111	-5.908	0.7071
	Bao 19C	Dark grey micrite			3.873	-5.182	–
	Bao 22V	White fine-grained calcite veins	4784.48	P ₁ m ¹	4.108	-5.146	0.7071
	Bao 22C	Dark grey micrite			3.817	-4.727	–
Jian 38	J38-6V	Grayish-white calcite veins	3151.42	T ₁ f ²	4.07	-7.113	0.7075
	J38-6C	Dark grey micrite			4.497	-5.105	–
	J38-9V	Grayish-white fine-medium grained calcite veins	3153.2		3.748	-6.611	0.7075
	J38-9C	Grey calcarenite			3.956	-6.401	0.7076

4 Organic geochemical tracers in marine strata

The western Hubei–eastern Chongqing area has four sets of source rocks. They are the lower Silurian, lower Cambrian, Permian coal-measures, and Permian carbonate. The lower Cambrian source rocks of the Qiongzhusi Formation in the east Sichuan Basin are mainly grayish black shale with maximum, minimum and average total organic carbon (TOC) values of 4.78%, 0.21%, and 1.38%, respectively. In addition, 102 samples (65% of the total 154 samples) have a TOC value above 0.5%. The hydrocarbon generation potential value of the Cambrian source rocks in immature and lower mature stage is between 0.5 mg/g and 20 mg/g. In the lower part, high-quality source rocks have a TOC value above 2.0% and a hydrocarbon generation potential value between 2 mg/g and 35 mg/g. The R_o of the source rocks is between 1.2% and 5.0% with an average at 3.0% reaching the overmature stage.

The Silurian source rocks of the Longmaxi Formation in the Shizhu-Xianfeng-Laifeng area are well developed with an abundance of organic matter. Most (102) of the samples have a TOC value above 1.0%; the average TOC value of the source rocks is 2.73%. The source rocks have a hydrocarbon generation potential value between 2 mg/g and 35 mg/g, which is higher in the northern part than in the southern part. The R_o in Silurian rocks in the study area is between 2.0% and 3.0%.

The Permian source rocks include the coal-measures and carbonates. 390 shale samples in the western Hubei–eastern Chongqing area have an average TOC value of 2.71%. The samples of poor source rock with a TOC between 0.5% and

1.0% account for 10% of all samples; those of medium-good source rock with a TOC between 1.0% and 4.0% account for 63% of all samples; and those of excellent source rock with a TOC above 4.0% account for 22% of the samples. In the Shizhu-Lichuan area, the R_o of the shale source rock is generally above 2.0%, indicating a dry gas stage. The Permian carbonate source rocks have been seldom studied and are considered as minor source rocks.

After analyzing the characteristics of the four sets of source rocks in the study area, we were able to define the origin of the hydrocarbon in the main production formations by studying the biomarker characteristics of the organic matter filling the fractures. In addition, we traced the origin of the fluid by studying the strontium, carbon, and oxygen isotopes of the veins of calcite, dolomite, and gypsum filling fractures. We also identified the hydrocarbon accumulation period and the reservoir forming time through examination of inclusions.

4.1 Organic geochemical tracer in the marine strata of Xinchang structure

Coring was performed only in well Xinchang 2 of the Xinchang structure so drill core from this well was the only intact samples available. Tables 1 and 2 demonstrate the distribution of the residual organic matter from the source rocks and reservoirs.

Chromatography from the three samples (XC2-22s, XC2-23s, XC2-25s) of Permian source rocks showed a unimodal distribution of saturated hydrocarbons from high to low, of which the ratio between low *n*-alkanes and high *n*-alkanes was 1.34, 2.22, and 1.56, respectively (Fig. 3, Table 1). The

ratio between isoprenoid hydrocarbon and the corresponding *n*-alkane was either dominated by *n*-alkane or isoprenoid hydrocarbon. In XC2-22s, the sample of coal-measure source rocks in the Qixia Formation, Ts/Tm was 0.90; $C_{29}Ts/(C_{29}Ts+C_{29})$ was 0.18; gammacerane/ C_{30} hopane was 0.19; tricyclic terpane/ C_{30} hopane was 3.33; relative content of C_{21} and C_{22} pregnane was 2.62; and the ratio between diasterane and regular sterane was 0.28. In XC2-14s, a sample of carbonate source rocks in the Changxing Formation, Ts/Tm was 0.50; $C_{29}Ts/(C_{29}Ts+C_{29})$ was 0.18; gammacerane/ C_{30} hopane was 0.29; tricyclic terpane/ C_{30} hopane was 0.26; relative content of C_{21} and C_{22} pregnane was 0.09; and the ratio between diasterane and regular sterane was 0.06 (Table 2). Therefore there are at least two different sets of Permian source rocks. These are the Permian coal-measure source rocks in the Qixia Formation and Permian carbonate source rocks in the Changxing Formation. The residual organic matter in the pores of the Permian reservoirs, XC2-20, showed a unimodal distribution in saturated hydrocarbon chromatography with a ratio of low-*n* to high-*n* carbon of 1.37, significantly dominated by low-*n* carbon. In addition, the sample was dominated by *n*-alkane according to the ratio of isoprenoid hydrocarbon and *n*-alkane. In this sample, Ts/Tm was 0.93; $C_{29}Ts/(C_{29}Ts+C_{29})$ was 0.28; gammacerane/ C_{30} hopane was 0.19; tricyclic terpane/ C_{30} hopane was 1.71; relative content of C_{21} and C_{22} pregnane was 1.02; and the ratio between diasterane and regular sterane was 0.20 (Table 2). The biomarker distribution of terpane and sterane showed that the residual organic matter in the pores of the Permian reservoirs was sourced from Permian coal-measure source rocks.

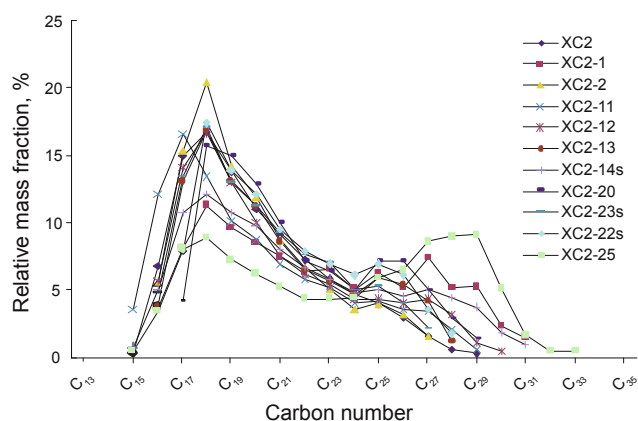


Fig. 3 *n*-alkane distribution characteristics of marine strata samples from well Xinchang 2

Chromatography of organic matter filling the suture zone in the Feixianguan Formation in well Xinchang 2 (XC2-11, 12, 13) showed a unimodal distribution in saturated hydrocarbon. The ratio between low-*n* and high-*n* carbon was 2.49, 2.01, and 1.99 in the three samples, showing significant characteristics of lighter alkanes (Table 1). *n*-alkane was essentially dominant in the ratio between isoprenoid and *n*-alkane, and phytane was dominant in the ratio between pristane and phytane, which is a similar trend to that of the Permian carbonate source rocks. However, the terpane and sterane biomarker parameters of the residual organic matter from the three samples from the Feixianguan Formation

showed two different types of characteristics (Fig. 4, Table 2). In XC2-11, for example, Ts/Tm was 0.56; $C_{29}Ts/(C_{29}Ts + C_{29})$ was 0.25; gammacerane/ C_{30} hopane was 0.26; tricyclic terpane/ C_{30} hopane was 0.49; relative content of C_{21} and C_{22} pregnane was 0.23; and the ratio of diasterane and regular sterane was 0.07, showing a similar trend to that of the Permian carbonate source rocks. However, the biomarker parameters of XC2-12 showed characteristics similar to those of Permian coal-measure source rocks, of which Ts/Tm was 0.73; $C_{29}Ts/(C_{29}Ts + C_{29})$ was 0.14; gammacerane/ C_{30} hopane was 0.26; tricyclic terpane/ C_{30} hopane was 2.02; relative content of C_{21} and C_{22} pregnane was 1.15; and the ratio of diasterane and regular sterane was 0.14 (Table 2). Moreover, some biomarker parameters of this residual organic matter also showed similar characteristics to those from Permian carbonate source rocks, such as Ts/Tm and diasterane/regular sterane.

Analysis of aromatic biomarkers in well Xinchang 2 (Table 3) showed that Permian coal rocks in the Qixia Formation and carbonate rocks in the Changxing Formation had a phenanthrene content of 77.8%-93.5%, approaching that of organic matter in the Triassic reservoirs of the Feixianguan Formation, which was 84.2%-99.5%. Among dibenzothiophene, dibenzofuran, fluorene and their homologues, the fluorene content was similar, while differences exist in the contents of dibenzothiophene and dibenzofuran. However, no great differences exist in F/DMF (fluorene/dimethylfluorene), SF/P (dibenzothiophene/phenanthrene), or F + MF + OF/DMF + DOF + SF (fluorene + methylfluorene + dibenzofuran) / (dimethylfluorene + dimethyldibenzofuran + dibenzothiophene) ratios of the organic matter in Permian source rocks and Triassic reservoirs, while the organic matter in the Triassic reservoirs exhibited characteristics of Permian source rocks.

Therefore, the hydrocarbon sources of residual organic matter in the Triassic reservoirs of the Feixianguan Formation were from Permian carbonate rocks and mixed coal-measure source rocks. However, saturated hydrocarbon chromatography proved that the three samples underwent a certain degree of biodegradation, indicating that the preservation conditions of these samples had been damaged in the geological history.

The organic sample XC2-25 from a Carboniferous reservoir showed a bimodal distribution in saturated hydrocarbon chromatography, of which the ratio of low-*n* and high-*n* carbon was 0.67, indicating high-*n* alkanes dominate. The pristane/ nC_{17} ratio was 0.7 with dominant nC_{17} ; the phytane/ nC_{18} ratio was 1.03 with dominant phytane; and the pristane/phytane ratio was 0.61 with dominant phytane. The saturated hydrocarbon chromatography of this sample showed characteristics similar to that of Silurian source rocks (Xu et al, 2009), but certain differences exist. Silurian source rocks are dominated by high-*n* alkanes with saturated hydrocarbon chromatography from low to high, while that of XC2-25 was from high to low with characteristics similar to that of Cambrian source rocks. The terpane and sterane biomarker parameters of this sample, including tricyclic terpane/ C_{30} hopane, relative content of C_{21} and C_{22} pregnane, and diasterane/regular steranes, differed significantly from those

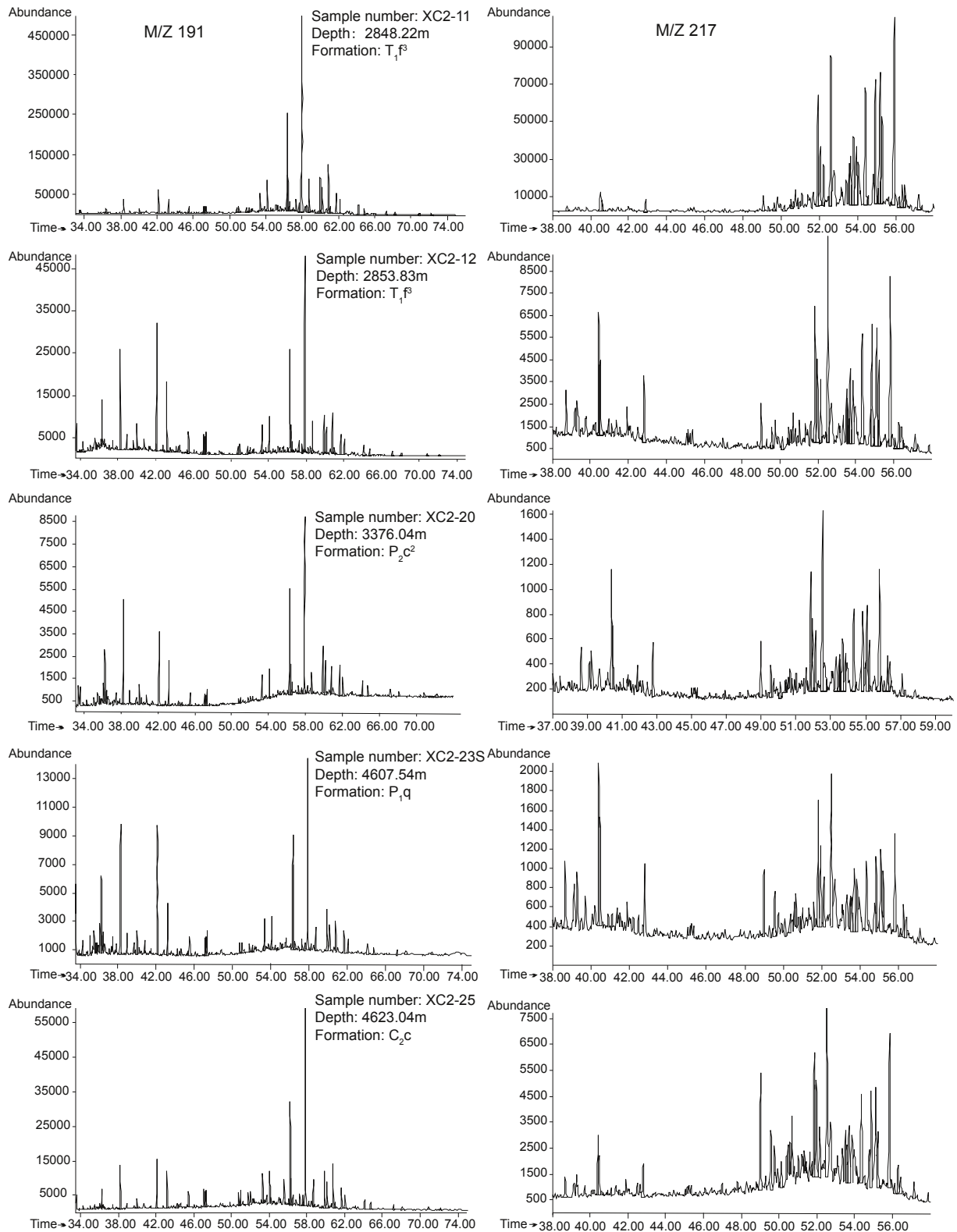


Fig. 4 Terpene and sterane biomarker diagram of samples from well Xinchang 2

observed in Permian source rocks.

We consider that the main hydrocarbon sources of the Carboniferous reservoirs in well Xinchang 2 were Silurian and Cambrian source rocks. Severe biodegradation occurred in the sample; thus, preservation conditions of the petroleum system were damaged. The present organic

geochemical characteristics evident in the sample show that the Carboniferous and Permian rocks once were part of two different fluid systems; that is, Permian rocks and the underlying strata were completely disconnected before the hydrocarbon generated in Cambrian source rocks migrated to the Carboniferous rocks.

4.2 Organic geochemical tracers in the marine strata of the Longjuba structure

Methane is the dominant natural gas component of the Permian Maokou Formation in the well Long 8, Longjuba structure, accounting for 98.35%; N₂ and CO₂ were second and third, respectively. The content of ethane was lower at 0.14%; no H₂S was detected (Table 4).

The carbon isotopes of the CH₄ is influenced by the types of the source rocks in addition to maturity, which results in an overlap of the δ¹³C₁ distribution interval of coal-type and oil-type gases, classified as humic and sapropelic, respectively. As a result, it is difficult to determine the difference between these gas types using δ¹³C₁. The carbon isotope ratio in heavy hydrocarbons of natural gas, such as ethane, is more stable. This can accurately reflect the types of gas-generating materials. By examining criteria based on the carbon isotope analysis of 283 continental and marine samples from 8 basins in China (Shi et al, 2000; Xu et al, 1997; Dai, 1992; Zhang et al, 1987; 1988) in addition to research data of the natural gas in marine sediments in the Tarim Basin (Zhao et al, 2001; Liang et al, 2002; Xie et al, 1999), we estimated the genetic types of natural gas (Table 7).

The carbon isotope analysis of the natural gas from the well Long 8 in P₁m Formation indicates that the natural gas is overmatured dry and sapropelic gas (Table 5), with a high methane carbon isotope ratio. From the crossplot of δ¹³C₁ and δ¹³C₂ (Fig. 5), it can be seen that the natural gas from the well Long 8 P₁m Formation and the natural gas from P₁m, P₂ch and T₁f³ formations in eastern Sichuan are basically distributed in the same area in the cross-plot, which indicates that the Permian source rocks have also made some contribution to the formation of natural gas from the P₁m Formation in well Long 8. The cause of the reversal of methane and ethane ratios might be the mixing of different natural gases from different source rocks.

Table 7 The classification of carbon isotopes in marine natural gas

Types		δ ¹³ C ₂ , ‰	δ ¹³ C ₁ , ‰
Sapropelic	mature	<-34.0	<-40
	overmature		>-40
Humic-bearing	mature	-34.0 - -29.5	<-40
	sapropelic		>-40
Humic	mature	>-29.5	<-32
	overmature		>-32

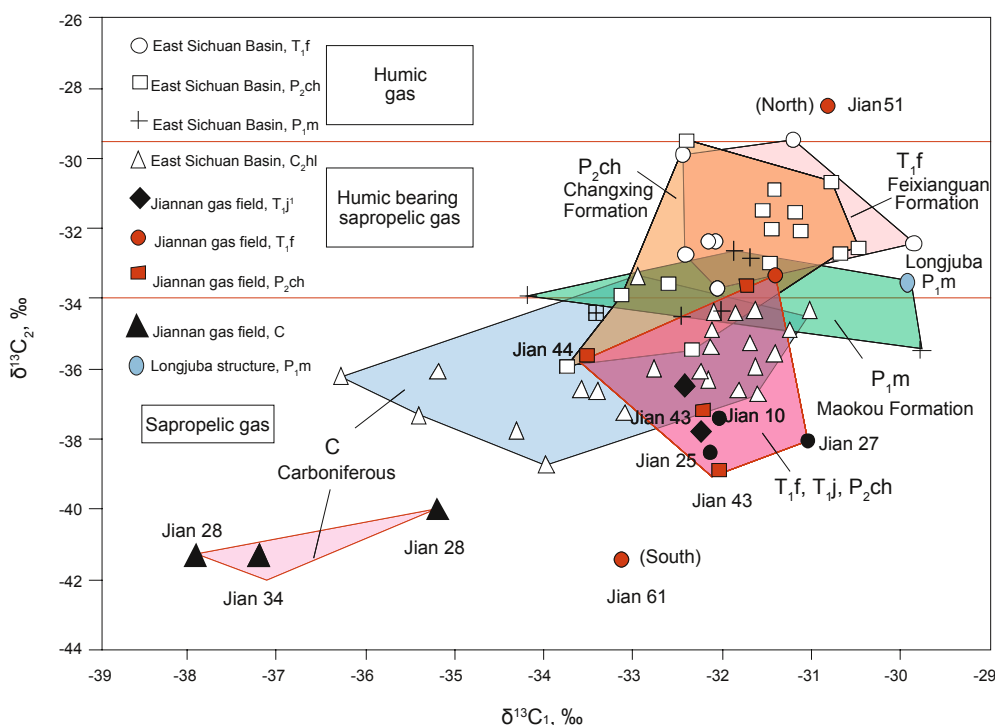


Fig. 5 Methane and ethane carbon isotope ratios of natural gas in the Longjuba structure, Jiannan gas field and eastern Sichuan Basin

Through the matrix-source-judging formula proposed by Pang et al (2000), with the methane carbon isotopes and the components of the natural gas from the well Long 8, the gas type index (GTI) and kerogen type index (KTI) are obtained and listed as follows: the GTI is 0.339; the KTI is 67.0. All the data indicate that the natural gas originated from the relatively high-quality source rocks. On the basis of our

calculation, the maturity of the source rocks is 2.6%-4.05%, with an average value of 3.2%. The asphalt reflectance of the dark-grey bioclastic limestones at a depth of 4,786.92 m in the well Long 8 of the 1st section of the Permian Maokou Formation is 3.03%. After conversion, its vitrinite reflectance is 2.27%. The calculated maturity of the source rocks which formed the methane found in the well is not in agreement

with the measured maturity of the source rocks from the Permian Maokou Formation but it is closer to the maturity of the source rocks from the Silurian mudrocks. The vitrinite reflectance of the source rocks from the Silurian in the study area is 2.5%-3.5% (Liu et al, 2002). The natural gas from the Long 8 well in P₁m Formation is a mixed product from both Silurian mudstones and Permian carbonates sources.

4.3 Organic geochemical tracers in marine strata of the Jiannan structure

The natural gas drying coefficient (C_1/C_1-C_5) of the four production formations (Jialingjiang, Feixianguan, Changxing and Huanglong) in Jiannan gas field is above 98.5% with a maximum value of 99.9% indicating an overmature dry gas. The natural gas in Carboniferous rocks has a relatively high C_2 content with a small quantity of C_3 (0.13%-0.24%), and its CO_2 and H_2S contents are both below 4.5% (Table 4). The compositions of natural gas in various horizons of the Jiannan gas field were basically the same with a high content of methane and low contents of ethane, propane, and other heavy hydrocarbon components, showing it is post-mature pyrolysis gas. However, such component characteristics are unable to reflect differences in genesis.

The isotope ratios of methane in the natural gas from the P₁m, P₂ch and T₁f³ formations in the Jiannan gas field are high, between -31‰ and -33‰, which indicates that the evolutionary degree of the natural gas is high. In comparison, their ethane isotopes are widely distributed, with striking differences being displayed in the high points of the south and the north. The $\delta^{13}C_2$ in the high point of the north is heavier, with an average value of -33.7‰, which suggests that most of the natural gas is from humus-bearing sapropels, with only a few exceptions, some of which might be sapropelic gas. The $\delta^{13}C_2$ in the high point of the south is lighter, with an average value of -38.8‰, which suggests that the natural gas is sapropelic gas (Fig. 5 and Table 5). All the data indicate that the genesis and the sources of the natural gas are complicated. From the crossplot of $\delta^{13}C_1$ and $\delta^{13}C_2$ (Fig. 5), it can be seen that the distribution of carbon isotopes of the natural gas from the P₂ch and T₁f³ formations in the Jiannan gas field and the distribution of carbon isotopes of the natural gas from the Carboniferous in eastern Sichuan basically overlap but some differences are shown in the distribution of the carbon isotopes of the natural gas from T₁f and P₂ch formations in the other parts of the area. As the natural gas in the Carboniferous in eastern Sichuan is mainly from sapropelic source rocks from the lower part of the Silurian system (Dai et al, 2010), the natural gas from the P₂ch and T₁f³ formations in the Jiannan gas field is also mainly from source rocks of the lower part of the Silurian system. However, the contribution of source rocks from the Permian system cannot be ignored. The higher ethane carbon isotope ratios of the gas samples from the north points of P₂ch and T₁f³ formations indicate a greater contribution from the Permian source rocks. Humic gas is even found in the well No.51 in T₁f³ Formation of Jiannan gas field. The reversal of the carbon isotopes of the gas from P₂ch and T₁f³ formations of Jiannan gas field mostly occurs, the only difference being the degree. Some scholars maintain that

such a reversal is due to a higher degree of maturity. Instead, we consider it is due to the mixing of sources.

The carbon isotopes of the natural gas generated from Carboniferous of Jiannan gas field are lighter. The average value of the $\delta^{13}C_1$ is -36.8‰ and the average value of the $\delta^{13}C_2$ equals to or is less than -40‰, which is obviously lighter than those of the natural gas samples from the Permian, the Triassic and the Carboniferous of eastern Sichuan. The natural gas in eastern Sichuan is mainly generated from Silurian source rocks (Zhu et al, 2006). The natural gas from the Carboniferous of Jiannan might be the product of the mixing of gas from other source rocks, such as the Cambrian source rocks, at the deeper part or the other parts of the formation. The reversal of the carbon isotope of the natural gas also occurs.

To study the source rocks in greater detail, we used the carbon isotope values of the kerogen in various sets of source rocks in the east Sichuan Basin and compared them with the $\delta^{13}C_1$ of natural gas in the Jiannan gas field (Fig. 6). The kerogen in limestone samples of P₁l, P₁q, P₁m, and P₂w was a mixed-type with the average $\delta^{13}C_{kerogen}$ between -26.8‰ and -28.3‰, which is 3.8‰-4‰ heavier than the $\delta^{13}C_1$ value in T₁f³ in the northern high point (-30.8‰ - -32.1‰), which corresponds to the fractionation during the alteration from kerogen to CH_4 . The natural gas of the T₁f³ Formation in the northern high point originated from mixed-type source rocks classified as mainly sapropelic. The shale in P₂l, P₂w, and P₂d and the bioclastic limestone in P₂ch were humic with a significantly heavy $\delta^{13}C_{kerogen}$ value, the average of which was between -24.2‰ and -25.2‰. The $\delta^{13}C_{kerogen}$ value in these four formations was 7‰-8‰ heavier than the $\delta^{13}C_1$ value in the Permian and Triassic natural gas with the maximum at 10‰, indicating that these four formations are not the source of the Permian and Triassic natural gas in the Jiannan gas field. For this reason, it can be assumed that the natural gas from the Permian and the Triassic in the Jiannan gas field

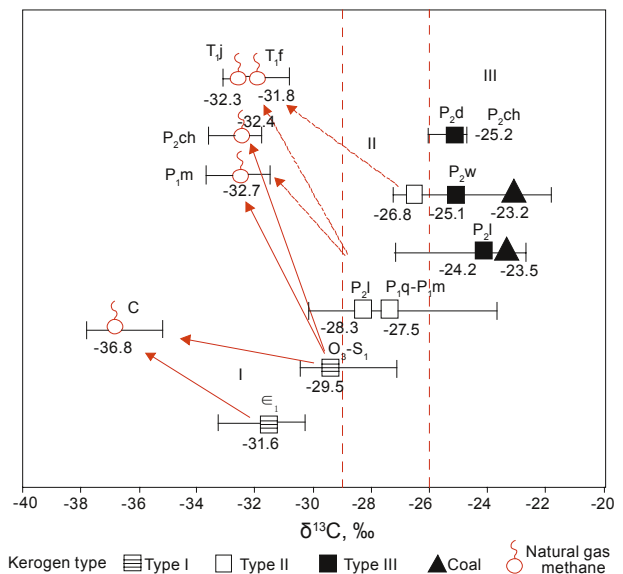


Fig. 6 Comparison of $\delta^{13}C_1$ of the natural gas in the Longjuba structure and Jiannan gas field and $\delta^{13}C_{kerogen}$ in source rocks in the eastern Sichuan Basin

is generated mainly from Silurian source rocks and part of it is generated from Permian mixed source rocks, mainly sapropelic source rocks. The Permian humus-bearing source rocks have made less contribution to the formation of the natural gas of the area. The average $\delta^{13}C_{kerogen}$ values of the kerogen in the Cambrian and Silurian are -31.6‰ and -29.5‰ respectively, so classified as sapropelic kerogen. The natural gas in the Carboniferous is typical sapropelic natural gas with its $\delta^{13}C_2$ value below -40‰; its gas sources are the sapropelic source rocks in the Cambrian and the Silurian.

Comprehensive analysis shows that the natural gas in the Jiannan gas field is mainly sapropelic; that the natural gas from P_2ch and T_1f^3 formations was mainly generated in Silurian source rocks, with Permian humus-bearing sapropelic source rocks as its secondary source. A specific sample from well No. 51 in T_1f^3 Formation of Jiannan gas field displays some relation with the Permian source rocks of the coal-

bearing series. The natural gas from the Carboniferous formations was mainly generated in the source rocks of the Silurian system and the Cambrian source rocks have also contributed to it.

5 Fluid migration paths

To more accurately trace the fluid migration paths, a profile was selected from Wanxian northwest to Xiaoqingya southeast that essentially includes the Fangdoushan and Qiyueshan fault zones, the Jiannan structure, and other tectonic zones (Fig. 7(a)). Through analysis of fluid migration paths of three typical structures—Xinchang 2, Long 8, and Jian 38 wells, hydrocarbon accumulation and migration were examined, the formation, evolution, destruction and modification of different structures were studied, and hydrocarbon preservation conditions were evaluated in this area.

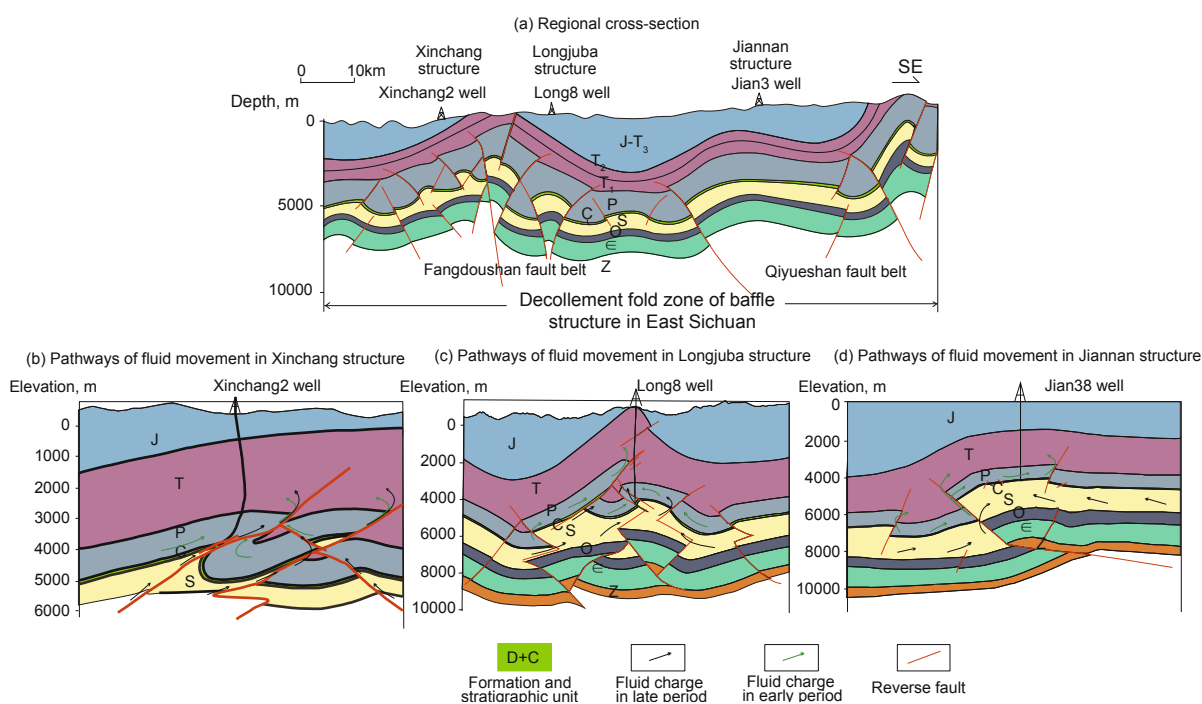


Fig. 7 Fluid migration paths in marine strata of the western Hubei–eastern Chongqing area

5.1 Fluid migration path in Xinchang structure

The $^{87}Sr/^{86}Sr$ value of normal paleo-seawater in the Early Triassic (the similar sedimentary age of Jialingjiang Formation) simulated by McArthur (1994) and Korte et al (2005a; 2005b) ranged from 0.7076 to 0.7082; that of seawater (the similar sedimentary age of Daye Formation) simulated by Reinhardt et al (1998) and Veizer et al (1999) ranged from 0.7076 to 0.7078; and that of Early Permian normal seawater ranged from 0.7076 to 0.7082. Analysis was performed on strontium isotopic composition and evolution of Late Permian–Early Triassic seawater in marine carbonate rocks in Zhongliangshan, Chongqing, reported by Huang et al (2008). The conclusions were consistent with those published by Korte et al (2003; 2005a; 2005b), proving that the criterion

of strontium isotopic ratio used in this study is applicable to rocks in southern China.

According to studies on carbon, oxygen, and strontium isotopes in the Permian Changxing Formation of well Xinchang 2 (Table 6), significant differences were observed in the oxygen isotopes and weak differences were observed in carbon isotopes. These studies implied that the fluids leading to vein formation were not sourced from the products of adjacent surrounding rocks after redissolution. However, the $^{87}Sr/^{86}Sr$ value of gypsum filling spaces in the Permian Changxing Formation (0.7100) was close to the strontium isotope of Early Cambrian seawater, which was reported as 0.7087-0.7100 (Burke et al, 1982; Denison et al, 1994; Shi et al, 2002; Korte et al, 2003). These results indicate that fluids leading to the formation of gypsum were sourced from lower

Cambrian strata.

Previously accumulated calcium-carbonate-rich fluids were sourced from Permian rocks with abundant organic inclusions (Fig. 9(a)), indicating that the Permian source rocks reached the peak of hydrocarbon generation at this stage. The homogenization temperature peaks of coexisting saline inclusions were 120-130 °C and 160-190 °C (Fig. 9(b)), corresponding to the depths of hydrocarbon migration and accumulation at 3,333-3,667 m and 4,666-5,667 m, respectively. According to the hydrocarbon generation history of Upper Permian source rocks simulated by the Easy% R_o chemical kinetic model (Fig. 10(a)), the R_o value of source rocks ranged from 0.65% to 0.70% in the middle Late Triassic; the rocks were buried 3,450 m in this stage of abundant hydrocarbon generation. In the initial Early Jurassic, the maturity of the source rocks was about 1.00%, at which stage hydrocarbon generation reached its peak. In the middle Early Jurassic, the maturity of source rocks was 1.35%, at which stage gas generation occurred. In the late Early Jurassic, R_o value was 2.0%, at which stage significant gas generation occurred in Permian source rocks. Meanwhile, inclusion characteristics and homogenization temperatures also show that two-stage hydrocarbons were captured in Permian reservoirs (P_2ch^2) in the initial and the late epochs of the Early Jurassic.

Residual biomarker characteristics of organic matter obtained from the fractures of the third member of Feixianguan Formation, show its source was Permian source rocks. The time of formation of the organic matter filling the reservoir fractures should be equivalent to the capture time of vein inclusions in reservoir fractures of the lower Triassic Feixianguan Formation because both have the same set of source rocks (Fig. 8(a)).

The gypsum filling the reservoir fractures of the Permian Changxing Formation has been proved to be sourced from the underlying Cambrian. A large amount of water-soluble methane exists in the inclusions along indistinct fractures in gypsum (Fig. 9(c)), indicating that Cambrian source rocks evolved to hydrocarbon expulsion with a high maturity or to a generation stage of abundant dry gas. The vein-filling sequence shows the formation of gypsum was later than that of the calcite (Fig. 8(b)). A large amount of natural gas and calcium-sulfate-rich water generated in Cambrian source rocks migrated to the overlying Permian reservoirs, the main pathway of which was probably faults and fractures generated by Yanshan tectonism. In addition, the residual organic biomarkers along Carboniferous reservoir fractures have characteristics of Cambrian and Silurian source rocks.

At least two stages of fluid accumulation occurred in the Permian reservoirs of the Xinchang structure (Fig. 7(b)). At the early stage, the calcium-carbonate-rich fluid was sourced from the Permian and formed the calcite. At the late stage, the calcium-sulfate-rich fluid was sourced from the Cambrian and formed the gypsum. Moreover, the later accumulated fluids made certain modifications to the fluids charged earlier. Earlier hydrocarbon preservation conditions were damaged by the long-distance and large-scale cross-formational flow of fluids, leading to serious problems for oil and gas exploration in the Xinchang structure.

5.2 Fluid migration path in Longjuba structure

Analysis of carbon and oxygen isotopes from the Permian in the well Long 8, indicated that although carbon and

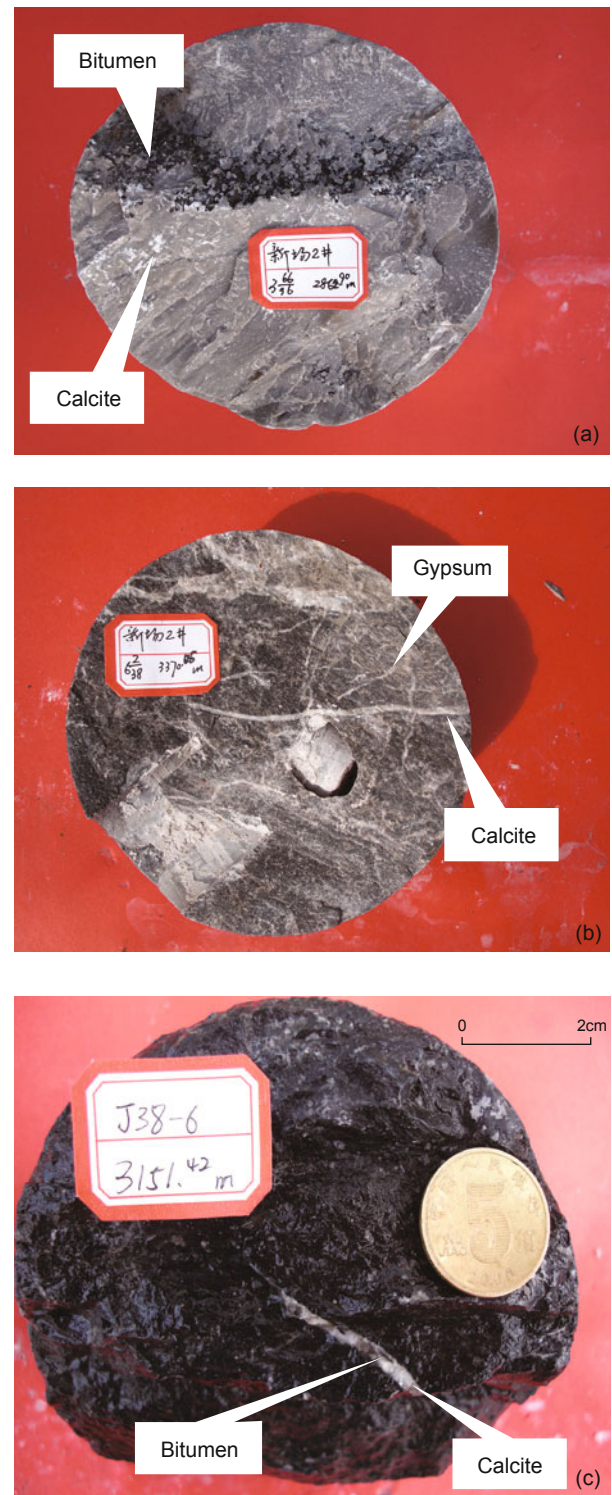


Fig. 8 Core photos of well Xinchang 2 and well Jian 38 (a) The vein-filling sequence of the reservoir in Lower Triassic, Feixianguan Formation (at the depth of 2,862.9 m) of the Xinchang 2 well (the calcite filled before the bitumen). (b) The vein-filling sequence of the reservoir in Upper Permian, Changxing Formation (at the depth of 3,370.05 m) of the Xinchang 2 well (the calcite filled before the gypsum). (c) The vein-filling sequence of the reservoir in Lower Triassic, Feixianguan Formation (at the depth of 3,151.42 m) of the Jian 38 well (the calcite filled before the bitumen)

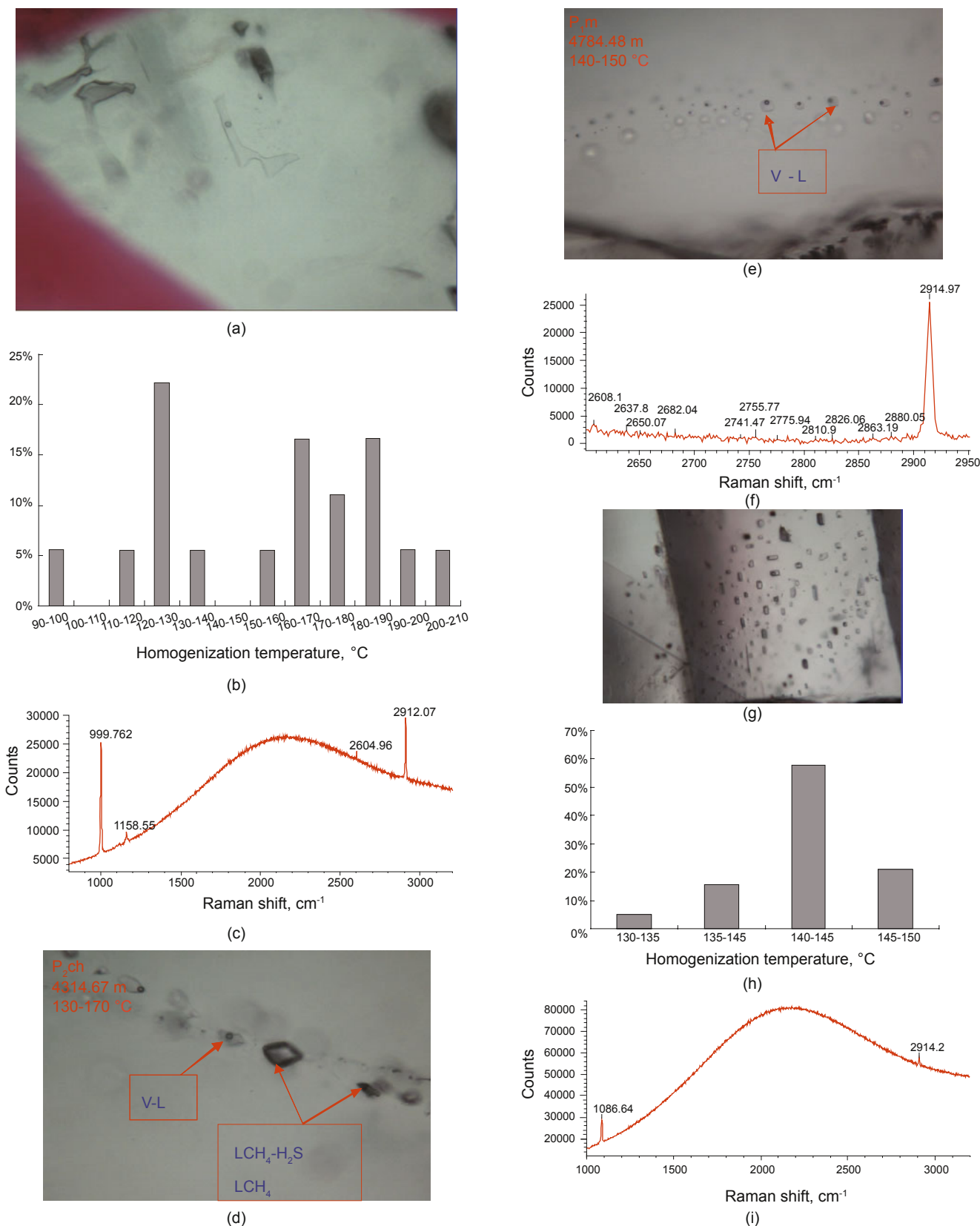
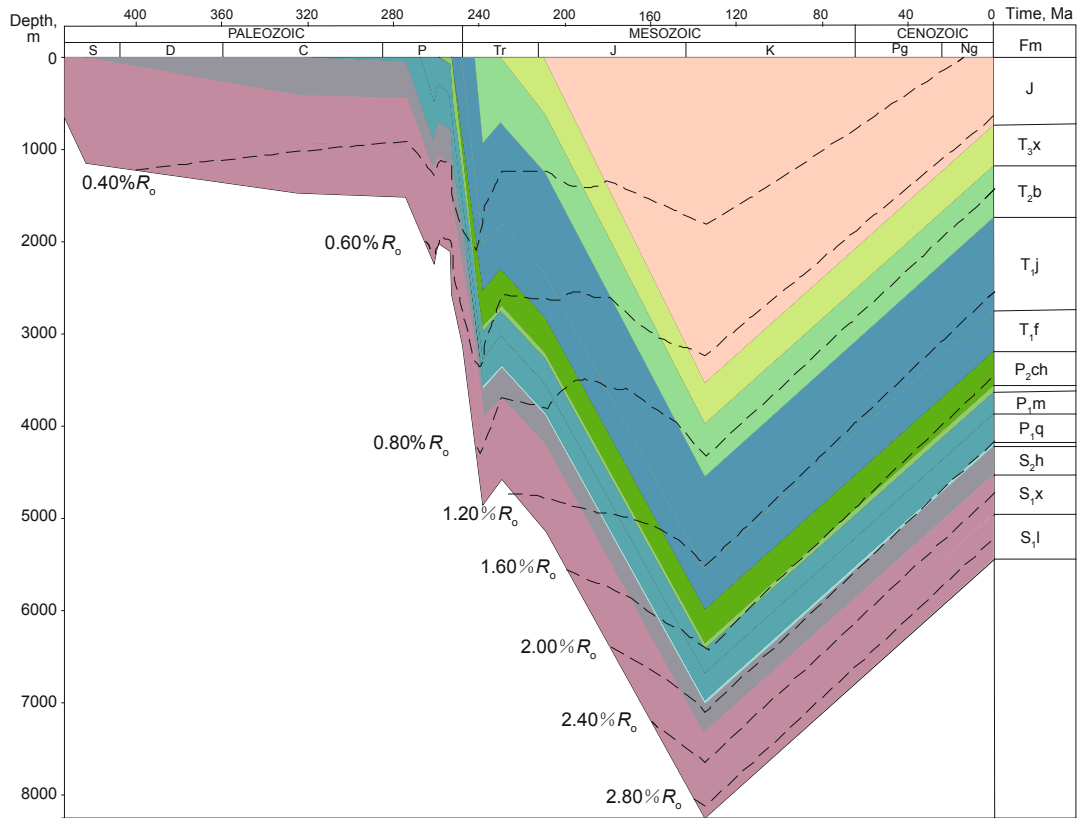
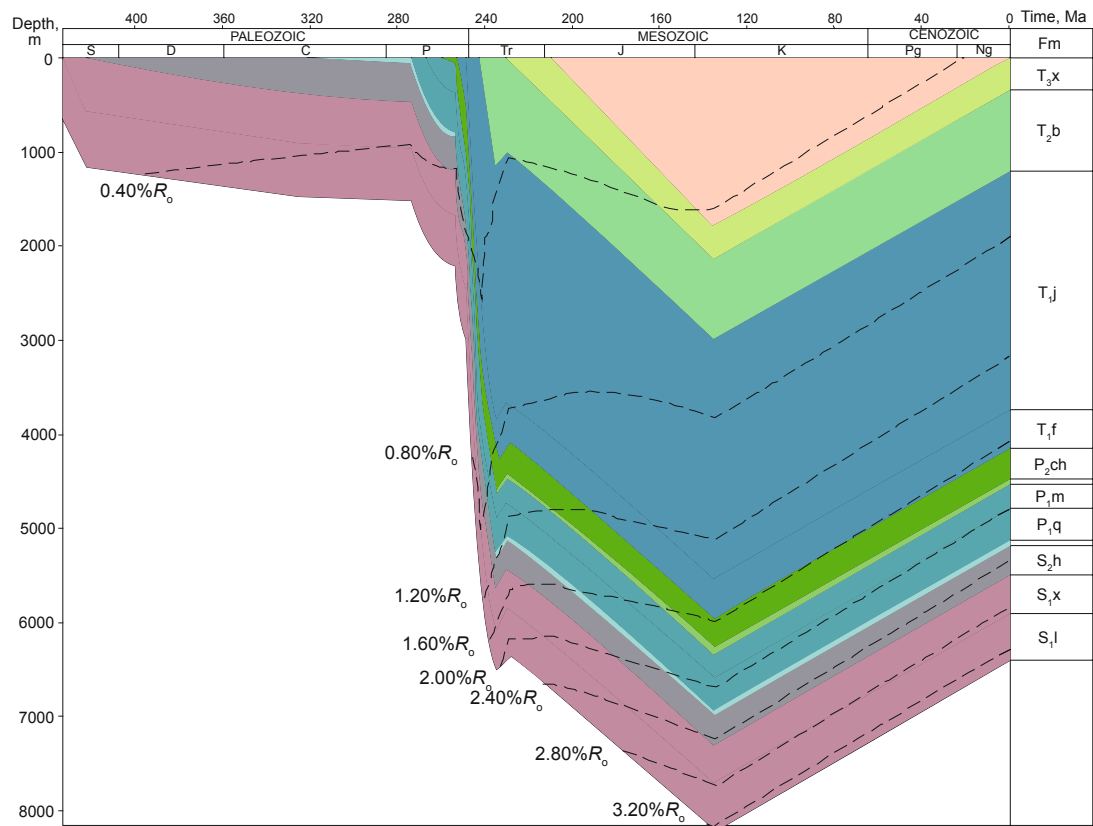


Fig. 9 Photos, homogenization temperature and laser Raman spectra of fluid inclusions (a) The organic fluid inclusions of calcite veins in Permian reservoir fractures of sample (XC2-18, 3,373.55 m, P₂ch), Xinchang 2 well. (b) Homogenization temperature distribution diagram of fluid inclusions in calcite veins of Permian reservoirs (at the depth of 3,373.55 m) of the Xinchang 2 well. (c) Laser Raman spectra of organic inclusions in the second member of the Upper Permian Changxing Formation (P₂ch²) of the Xinchang 2 well. (d) Fluid inclusions in calcite veins filling reservoir fractures of the Changxing Formation, Long 8 well. (e) Fluid inclusions of calcite veins filling Permian reservoir fractures of the Maokou Formation, well Long 8. (f) Laser Raman spectra of organic inclusions in the veins of the Maokou Formation, well Long 8. (g) Gas-liquid saline inclusions coexisting with organic inclusions, which are dark-gray, single-phased and in the shape of rectangle. Saline inclusions are liquid- and gas-phased; horizon: T₁f³, depth: 3,153.20 m, well: Jian 38. (h) Homogenization temperature distribution diagram of fluid inclusions in the third member of the Lower Triassic Feixianguan Formation (T₁f³) of the well Jian 38. (i) Laser Raman spectra of organic inclusions in the third member of Lower Triassic Feixianguan Formation (T₁f³) of the well Jian 38; 2914.2 cm⁻¹ and 1086.64 cm⁻¹ refer to CH₄ and calcite, respectively, in this figure



(a)



(b)

Fig. 10 Burial history and hydrocarbon generation history of source rocks

oxygen isotopes of veins and surrounding rocks ranged in the scope of normal seawater during the same period, $\delta^{13}\text{C}$ and $\delta^{18}\text{O}$ of $\text{P}_{1\text{m}}$ ranged from -2‰ to 6‰ and from 6‰ to 0‰,

respectively; those of P_{2ch^2} ranged from -1.5‰ to 4.5‰ and from -6.5‰ to 0‰, respectively (Korte et al, 2005a; 2005b). However, significant differences exist in carbon and oxygen

isotopes between Permian veins and surrounding rocks (Table 6). It was shown that the fluids leading to the formation of veins were not directly sourced from the fluids of adjacent surrounding rocks. The fluids filling the fractures of the Maokou Formation (P₁m) and Changxing Formation (P₂ch²) had ⁸⁷Sr/⁸⁶Sr values of 0.7071, within the strontium isotope range of Late Permian seawater (Burke et al, 1982; Denison et al, 1994; Shi et al, 2002; Korte et al, 2003). This finding indicates that the fluids in Lower Permian were sourced from the overlying Upper Permian. The fluids in the Upper Permian were not directly sourced from adjacent surrounding rocks but from other parts in Permian reservoirs.

All fluids of veins filling Permian reservoirs of the well Long 8 were sourced from the Late Permian. The inclusions in calcite veins of Changxing Formation samples (4,314.67 m) consisted of gas-liquid saline, water-soluble CH₄-H₂S, and CH₄ inclusions (Fig. 9(d)). These results indicate that fluid accumulation occurred at the peak stage of hydrocarbon generation, at which time the homogenization temperature of coexisting saline inclusions ranged between 130 °C and 170 °C, corresponding to hydrocarbon migration and accumulation depths between 3,667 m and 5,000 m.

The fluid inclusions in calcite veins filling the reservoir fractures of the first member of the Lower Permian Maokou Formation (4,784.48 m) mainly consisted of gas-liquid organic inclusions (Fig. 9(e), (f)), at which time the homogenization temperature peak ranged between 140 °C and 150 °C and the hydrocarbon accumulation depth was estimated at between 4,000 m and 4,330 m. The hydrocarbon generation history of Permian source rocks in the Long 8 well (Fig. 10(b)), indicates that hydrocarbon generation occurred in Permian source rocks in the late Middle Triassic and reached the peak stage in the early Late Triassic with a corresponding *R*_o value of 1.0%. Gas generation began in the late Middle Jurassic with a corresponding *R*_o value of 1.35%. From the inclusion characteristics and homogenization temperatures, we deduce that hydrocarbons were primarily captured in the Permian reservoirs of the well Long 8 during the early Middle Jurassic. However, the composition and isotopic characteristics of natural gas in the Permian in this well suggest that the natural gas is mainly from Silurian and Permian source rocks. Therefore, multi-source and multi-stage hydrocarbons were captured in Permian reservoirs.

The Permian reservoirs of the Longjuba structure were mainly characterized by two-stage fluid accumulation (Fig. 7(c)). One stage was the accumulation process of the Upper Permian calcium-sulfate-rich fluids and liquid hydrocarbon fluids. Strontium, carbon, and oxygen isotopic characteristics of calcite veins filling the reservoir fractures of the Changxing and Maokou formations revealed that the fluids of calcite veins were mainly sourced from the Upper Permian, and the inclusions in calcite veins mainly consisted of gas-liquid inclusions. The fluid charge occurred at the peak of hydrocarbon generation, and hydrocarbons were sourced from the Upper Permian source rocks. Moreover, analysis of natural gas in Permian reservoirs revealed the other stage of fluid accumulation was mainly from Silurian source rocks and part from Permian source rocks. The time order of the two-stage fluid accumulation was unable to be determined

through petrography. The accumulation of Permian fluids was prior to that of hydrocarbons generated in the underlying Silurian source rocks. If the accumulation of hydrocarbons generated in these source rocks was earlier, then traces of Silurian fluids should be retained in the Permian calcite veins. Therefore, the accumulation of Silurian fluids was later from short-distance cross-formational migration of natural gas to the Permian reservoirs. Tectonism was not very intense, and the faults and fractures were only able to connect the Silurian and Permian fluids. The significantly deep Permian reservoirs and thick overlying gypsum-halite beds allowed hydrocarbon preservation conditions to partially remain in this structure. Exploration results have shown Longjuba to be a gas-bearing structure.

5.3 Fluid migration path in the Jiannan structure

Dry black bitumen was discovered in calcite veins filling micrite fractures adjacent to the third-member Lower Triassic Feixianguan Formation of the well Jian 38 in the Jiannan structure (3,151.42 m). The calcite was filled first, followed by bitumen, leading to a significant time order with a vein width of 2-4 mm. Carbon, oxygen, and strontium isotopes of veins and surrounding rocks in this formation were in the range of Early Triassic normal seawater (Table 6) (Burke et al, 1982; Denison et al, 1994), indicating no influence on these isotopes in surrounding rocks and veins. However, significant differences existed in carbon and oxygen isotopes between veins and surrounding rocks. The fluids leading to the formation of veins were probably sourced from external fluids rather than from the surrounding rocks. The ⁸⁷Sr/⁸⁶Sr value of the surrounding rocks (0.7076) was consistent with that of Early Triassic normal seawater (0.7076), which indicates that the surrounding rocks were not influenced by external fluids, while more strontium isotopic characteristics of seawater in the original sedimentation were retained. The ⁸⁷Sr/⁸⁶Sr value of veins (0.7075) was also close to the high value of ⁸⁷Sr/⁸⁶Sr in Late Permian seawater (0.7067-0.7076), indicating that the fluids leading to the formation of veins could be sourced from the Lower Triassic and the Upper Permian strata.

The fluid inclusions of calcite veins filling the surrounding limestone fractures of the third-member (T₁³) Lower Triassic Feixianguan Formation (3,153.20 m) mainly consisted of gas-liquid and organic inclusions (Fig. 9(g)). The gas-liquid fluid inclusions were 3-12 μm in size, and the homogenization temperature ranged between 132 °C and 148 °C (the homogenization temperature peak ranged between 140 °C and 145 °C (Fig. 9(h))). Temperature measurement and laser Raman spectroscopy revealed that the organic inclusions mainly consisted of water-soluble methane (Fig. 9(i)), while H₂S was contained in some inclusions. Calcite veins were rich in water-soluble methane inclusions but lacked liquid petroleum inclusions. Thus, the charge of fluids leading to the formation of calcite veins likely occurred after petroleum pyrolysis. Calcite was mainly distributed at the fracture edges, and sparse dry bitumen was distributed in the center of the fractures. Thus, the bitumen in the center of fractures likely entered the fractures at the same time as the fluids leading to the formation of calcite, finally settling in the residual space

(Fig. 8(c)).

Analysis of carbon, oxygen and strontium isotopes of veins and surrounding rocks in the Lower Triassic Feixianguan Formation revealed that the original fluids leading to the formation of veins were most likely sourced from the Lower Triassic or Upper Permian. However, the Lower Triassic Feixianguan had no potential for hydrocarbon generation, indicating that the water-soluble methane filling the fractures were likely sourced from other strata below the Feixianguan Formation. Drilling data from the Jiangnan Oilfield indicate that natural gas was discovered in both the underlying Upper Permian and Lower Permian strata, showing that the natural gas in Feixianguan gas reservoirs could have the same hydrocarbon source as that of the underlying Permian reservoirs.

On the basis of the above analysis, gas sources of the Permian and Triassic natural gas in Jiannan gas field mainly include Permian carbonate source rocks and coal-measure source rocks in addition to Silurian source rocks. Therefore, in the case of earlier favorable preservation conditions, vertical migration occurred in part of the natural gas generated in the Silurian source rocks but did not reach the entire Feixianguan and Jialingjiang formations in the Lower Triassic. Most of the fluid charge occurred only in the overlying Carboniferous Huanglong Formation.

Traces of two-stage fluid migration and accumulation were observed in the Jiannan gas field (Fig. 7(d)). One stage of fluid migration was the accumulation of calcium-carbonate-rich fluids with Permian rocks as their source. At the same time, a significant amount of liquid hydrocarbons generated in Permian source rocks migrated to the Triassic reservoirs. No obvious accumulated traces of fluids existed in other horizons, while a favorable source-reservoir assemblage was formed among the Permian source rocks and the Permian and Triassic reservoirs. The other stage of fluid migration was shown as the accumulation of hydrocarbons into the overlying Carboniferous reservoirs mainly generated in the Silurian

source rocks. A favorable source-reservoir assemblage was formed between Silurian source rocks and Carboniferous reservoirs, resulting in an additional independent fluid system. In the Jiannan structure during Yanshan and Himalayan tectonism, the traps of various horizons remained intact, and no long-distance cross-formational accumulation of Cambrian fluids occurred in the Permian reservoirs. Accordingly, the hydrocarbon preservation conditions were excellent, and Jiannan gas field was discovered with vertical development of gas reservoirs in the Carboniferous Huanglong, Permian Changxing, and the Triassic Feixianguan and Jialingjiang formations.

Through the study of organic geochemical tracers in marine strata of the three typical structures, the differences of the fluid movement have been fully recognized and the formation, evolution, modification and destruction of different structures have also been analyzed (Table 8). The later accumulation of the Silurian and Cambrian fluids occurred in the Carboniferous, Permian, and Triassic reservoirs. In the case of a long-distance and large-scale cross-formational migration occurring in deep Cambrian fluids, later accumulated fluids modified existing accumulated fluids, resulting in the reduction of preservation conditions of earlier accumulated hydrocarbons. This has created major problems for exploration in Permian strata in the Xinchang structure. In case of a short-distance cross-formational charge of Silurian fluids to the Carboniferous and Permian reservoirs, only local modification occurred to the earlier closed and complete preservation systems, which resulted in favorable hydrocarbon preservation conditions. Exploration has shown Longjuba is a gas-bearing structure. The Silurian and Cambrian fluid accumulation in the neighboring Carboniferous reservoirs did not reach the entire Permian reservoir; the Permian-Triassic and the Silurian-Carboniferous source-reservoir assemblages were classified as two non-interfering fluid systems with excellent hydrocarbon preservation conditions, leading to the exploration and discovery of the Jiannan gas field.

Table 8 The differences of the fluid migration in Xinchang, Longjuba and Jiannan structures and their exploration situations

Structures	The relation between the hydrocarbon and the source	Early fluid accumulation	Late fluid accumulation	Distance between the formation	Preservation	Exploration achievement
Xinchang	1) The Triassic residual organic matter comes from the Permian carbonate and coal-measure source rocks	Permian →Permian, Triassic	Cambrian→ Permian	A long-distance cross-formational	Overall destruction	None
	2) The Permian residual organic matter is from the Permian coal-measure source rocks					
	3) The Carboniferous residual organic matter is from the Silurian and Cambrian source rocks					
Longjuba	1) The Permian natural gas is from the Permian and the Silurian source rocks	Permian→Permian	Silurian→Permian	A short-distance cross-formational	Partial destruction	Small gas bearing pools such as Longjuba structure
Jiannan	1) The natural gas of the northern high point comes from the Permian source rocks	Permian→Triassic	Cambrian, Silurian →Carboniferous	The fluid accumulation from neighboring strata	No destruction	Gas pools in the Huanglong Formation of the Carboniferous, the Changxing Formation of the Permian, the Feixianguan and Jialingjiang formations of the Triassic (Jiannan gas field)
	2) The Permian and the Triassic natural gas is derived from the Silurian source rocks					
	3) The Carboniferous natural gas is from the Silurian source rocks with a small part from the Cambrian source rocks					

6 Conclusions

1) At least four sets of source rocks existed in the western Hubei–eastern Chongqing area: Permian marine carbonate and coal-measure source rocks and Silurian and Cambrian argillaceous source rocks. The natural gas and the residual organic matter in the Triassic and the Permian strata showed similar characteristics to those of the Silurian source rocks, the Permian marine carbonate source rocks and the coal-measure source rocks, while the natural gas and the residual organic matter in the Carboniferous reservoirs showed similar characteristics to those of the Silurian source rocks with a small part coming from the Cambrian source rocks.

2) At least two stages of fluid accumulation occurred in Carboniferous-Triassic reservoirs in the study area. Earlier marine strata above the Permian were shown with an accumulation of liquid hydrocarbons generating in the Permian source rocks to the Permian and the Lower Triassic reservoirs. This accumulation was considered as internal fluid flow within the same relatively complete preservation system. The later accumulation of the Silurian and Cambrian fluids occurred in the Carboniferous, Permian, and Triassic reservoirs. In the case of a long-distance and large-scale cross-formational migration occurring in deep Cambrian fluids, later accumulated fluids modified existing accumulated fluids, resulting in destruction of preservation conditions of earlier accumulated hydrocarbons. In case of a short-distance cross-formational charge of Silurian fluids to the Carboniferous and Permian reservoirs, only local modification occurred to the earlier closed and complete preservation systems. The Silurian and Cambrian fluid accumulation in the neighboring Carboniferous reservoirs did not reach the entire Permian reservoir; and the Permian-Triassic and the Silurian-Carboniferous source-reservoir assemblages were classified as two non-interfering fluid systems with excellent hydrocarbon preservation conditions.

3) On the basis of studies of fluid migration paths in marine strata and comparative analysis of the exploration results, it was shown that intense late tectonism causing long-distance and large-scale cross-formational migration of deep Lower Paleozoic fluids was critical to hydrocarbon preservation conditions in Upper Paleozoic and Mesozoic marine strata. Accordingly, the zones with less severe late tectonism in the western Hubei–eastern Chongqing area with no superimposition or modification of Upper and Lower Paleozoic fluids and an Upper Paleozoic zone with fluid charging from the Lower Paleozoic should be important target areas for future hydrocarbon exploration.

Acknowledgements

This work was sponsored by National Programs for Fundamental Research and Development (973 Program, 2012CB214805), and the National Natural Science Foundation (40930424).

References

Al-Meshari A A, Kokal S L, Jenden P D, et al. An investigation of PVT effects on geochemical fingerprinting of condensates from gas

- reservoirs. *SPE Reservoir Evaluation and Engineering*. 2009. 12(1): 88-95
- Barclay S A, Worden R H, Parnell J, et al. Assessment of fluid contacts and compartmentalization in sandstone reservoirs using fluid inclusions: An example from the Magnus Oil Field, North Sea. *AAPG Bulletin*. 2000. 84(4): 489-504
- Boreham C J, Golding S D and Glikson M. Factors controlling the origin of gas in Australian Bowen Basin coals. *Organic Geochemistry*. 1998. 29(1-3): 347-362
- Burke W H, Denison R E, Hetherington E A, et al. Variation of sea water $^{87}\text{Sr}/^{86}\text{Sr}$ throughout Phanerozoic time. *Geology*. 1982. 10(10): 516-519
- Chen H D, Pang L, Ni X F, et al. New brief remarks on hydrocarbon prospecting of marine strata in the middle and upper Yangtze region. *Petroleum Geology and Experiment*. 2007. 29(1): 13-18 (in Chinese)
- Chen M K. Exploration potential of natural gas in western Hubei–eastern Chongqing area. *Journal of Jiangnan Petroleum Institute*. 2003. 25(1): 27-29 (in Chinese)
- Dai J X. The identification of alkane gas. *Science in China (Series B)*. 1992. 2: 185-193 (in Chinese)
- Dai J X, Ni Y Y and Huang S P. Discussion on the carbon isotopic reversal of alkane gases from the Huanglong Formation in the Sichuan Basin, China. *Acta Petrolei Sinica*. 2010. 31(5): 710-717 (in Chinese)
- Dai S W, He Z A and Wang J Y. Thinking of Meso-Paleozoic hydrocarbon exploration in South China. *Oil and Gas Geology*. 2001. 22(3): 195-202 (in Chinese)
- Denison R E, Koepnick R B, Burke W H, et al. Construction of the Mississippian, Pennsylvanian and Permian seawater $^{87}\text{Sr}/^{86}\text{Sr}$ curve. *Chemical Geology*. 1994. 112(1-2): 145-167
- England W A and Mackenzie A S. Some aspects of the organic geochemistry of petroleum fluids. *Geologische Rundschau*. 1989. 78(1): 291-303
- England W A, Mackenzie A S, Mann D M, et al. The movement and entrapment of petroleum fluids in the subsurface. *Journal of the Geological Society*. 1987. 144(2): 327-347
- England W A, Muggerridge A H, Clifford P J, et al. Modelling density-driven mixing rates in petroleum reservoirs on geological time-scales, with application to the detection of barriers in the Forties Field (UKCS) (in the *Geochemistry of Reservoirs*). *Geological Society Special Publications*. 1995. 86: 185-201 (in Chinese)
- Fu Z R, Li Z J and Zheng D Y. Structural pattern and tectonic evolution of NNE-trending strike-slip orogenic belt in the border region of Hunan and Jiangxi province. *Earth Science Frontiers*. 1999. 6(4): 263-272 (in Chinese)
- Galimov E M, Prokhorov V S, Fedoseyev D V, et al. Heterogeneous carbon isotope effects in synthesis of diamond and graphite from gas. *Geochemistry International*. 1973. 10(2): 306-312
- Gao L. Analysis on prospects in western Hubei–eastern Chongqing region. *Southern China Oil & Gas*. 2004. 17(2): 49-52 (in Chinese)
- Guo Z F, Chen M K, Fu Y X, et al. Natural gas reservoiring conditions of Sinian and Cambrian from western Hubei to eastern Chongqing areas. *Journal of Southwest Petroleum University (Science & Technology Edition)*. 2008. 30(4): 39-42 (in Chinese)
- Hao F, Li S T, Gong Z S, et al. Thermal regime, interreservoir compositional heterogeneities, and reservoir-filling history of the Dongfang Gas Field, Yinggehai Basin, South China Sea: Evidence for episodic fluid injections in overpressured basins. *AAPG Bulletin*. 2000. 84(5): 607-626
- Huang S J, Qing H R, Huang P P, et al. The formation and evolution of seawater strontium isotopes from Late Permian to Early Triassic—Based on the research on carbonatite in Zhongliang Mountain, Chongqing. *Science in China (Series D: Earth Sciences)*. 2008. 12(3): 273-283 (in Chinese)

- Karlsen D A, Nedkvitne T, Larter S R, et al. Hydrocarbon composition of authigenic inclusions: Application to elucidation of petroleum reservoir filling history. *Geochimica et Cosmochimica Acta*. 1993. 57(15): 3641-3659
- Korte C, Jasper T, Kozur H W, et al. $\delta^{18}\text{O}$ and $\delta^{13}\text{C}$ of Permian brachiopods: A record of seawater evolution and continental glaciation. *Palaeogeography, Palaeoclimatology, Palaeoecology*. 2005a. 224(4): 333-351
- Korte C, Kozur H W and Veizer J. $\delta^{13}\text{C}$ and $\delta^{18}\text{O}$ values of Triassic brachiopods and carbonate rocks as proxies for coeval seawater and palaeotemperature. *Palaeogeography, Palaeoclimatology, Palaeoecology*. 2005b. 226(3-4): 287-306
- Korte C, Kozur H W, Bruckschen P, et al. Strontium isotope evolution of Late Permian and Triassic seawater. *Geochimica et Cosmochimica Acta*. 2003. 67(1): 47-62
- Liang D G, Zhang S C, Zhao M J, et al. The hydrocarbon formation period in Kuche Depression. *Chinese Science Bulletin*. 2002. S1: 55-63 (in Chinese)
- Liu G X, Tao J Y, Pan W L, et al. Genetic types of the natural gas in the northeast and the east of Sichuan Basin. *Petroleum Geology and Experiment*. 2002. 24(6): 512-516 (in Chinese)
- Liu H F, Xia Y P, Yin J Y, et al. Coupling mechanism of strike-slip orogen and basin. *Earth Science Frontiers*. 1999. 6(3): 121-132 (in Chinese)
- Liu X M, Guo Z F and Fu Y X. Exploration potential of natural gas of lower assemblage in southeast margin of middle Yangtze Block. *Geology and Mineral Resources of South China*. 2007. 1: 59-64 (in Chinese)
- Lu H Z and Guo D J. Progress and trends of research on fluid inclusions. *Geological Review*. 2000. 46(4): 385-391 (in Chinese)
- Ma L. *Geotectonics and Marine Oil and Gas Geology in South China*. Beijing: Geology Press. 2004. 461-462 (in Chinese)
- Mackenzie A S and Mckenzie D. Isomerization and aromatization of hydrocarbons in sedimentary basins formed by extension. *Geological Magazine*. 1983. 120(5): 417-470
- Mackenzie A S, Lewis C A and Maxwell J R. Molecular parameters of maturation in the Toarcian shales, Paris Basin, France—IV Laboratory thermal alteration studies. *Geochimica et Cosmochimica Acta*. 1981. 45(12): 2369-2376
- Mackenzie A S, Maxwell J R, Coleman M L, et al. Biological marker and isotope studies of North Sea crude oils and sediments. *Proceedings of the World Petroleum Congress*. 1984. 11(2): 45-56
- Masterson W D. *Petroleum filling history of central Alaska North Slope fields*. Dallas: University of Texas. 2001
- McArthur J M. Recent trends in strontium isotope stratigraphy. *Terra Nova*. 1994. 6: 331-358
- Pang X Q, Zhou H Y, Li J Q, et al. The quantitative identification model of the evolution degree of mixing natural gas source material and the application of this model. *Acta Petrolei Sinica*. 2000. 21(5): 21-26 (in Chinese)
- Reinhardt E G, Blenkinsop J and Patterson R T. Assessment of a Sr isotope vital effect ($^{87}\text{Sr}/^{86}\text{Sr}$) in marine taxa from Lee Stocking Island, Bahamas. *Geo-Marine Letters*. 1998. 18(3): 241-246
- Rowe D and Muehlenbachs K. Isotopic fingerprints of shallow gases in the Western Canadian sedimentary basin: Tools for remediation of leaking heavy oil wells. *Organic Geochemistry*. 1999. 30(8): 861-871
- Rückheim J and England W A. Organic geochemistry of petroleum reservoirs. *Society of Exploration Geophysicists, 59th Annual International Conference, Expanded Abstracts and Biographies*. SEG Abstracts. 1989. 59(2): 1350-1351
- Shi H, Huang S J, Shen L C, et al. Stratigraphical significance of the strontium isotopic curve of the upper Paleozoic of Sichuan and Guizhou. *Journal of Stratigraphy*. 2002. 26(2): 106-110 (in Chinese)
- Shi X, Sun D M, Qin S F, et al. Carbon isotopic characteristics of natural gas in the great-medium coal-formed gas fields of China. *Experimental Petroleum Geology*. 2000. 22(1): 16-21 (in Chinese)
- Sweeney J J and Burnham A K. Evaluation of a simple model of vitrinite reflectance based on chemical kinetics. *AAPG Bulletin*. 1990. 74(10): 1559-1570
- Ungerer P. State of the art of research in kinetic modeling of oil formation and expulsion. *Organic Geochemistry*. 1990. 16(1-3): 1-25
- Veizer J, Ala D, Azmy K, et al. $^{87}\text{Sr}/^{86}\text{Sr}$, $\delta^{13}\text{C}$ and $\delta^{18}\text{O}$ evolution of Phanerozoic seawater. *Chemical Geology*. 1999. 161(1-3): 59-88
- Waples D W. Time and temperature in petroleum formation: Application of Lopatin's methods to petroleum exploration. *AAPG Bulletin*. 1980. 64(6): 916-926
- Welte D H and Yalcin M N. Basin modelling—A new comprehensive method in petroleum geology. *Organic Geochemistry*. 1988. 13(1-3): 141-151
- Wu Y Y. The method and practice of sequence stratigraphic analysis in the nonmarine basins. *Petroleum Exploration and Development*. 1997. 24(5): 7-10 (in Chinese)
- Xie Z Y, Li J and Lu X W. An approach to the changing origin and classification of ethane carbon isotope in marine gas of Tarim Basin. *Petroleum Exploration and Development*. 1999. 26(6): 27-29 (in Chinese)
- Xu G S, Cao J F, Zhu J M, et al. Division of fluid compartments and the formation and evolution of oil and gas accumulation in the typical structures of western Hubei—eastern Chongqing area, China. *Journal of Chengdu University of Technology (Science & Technology Edition)*. 2009. 36(6): 621-630 (in Chinese)
- Xu Y C, Shen P, Tao M X, et al. Geochemistry on mantle-derived volatiles in natural gases from eastern China oil/gas provinces (I): A novel helium resource—commercial accumulation of mantle-derived helium in the sedimentary crust. *Science in China (Ser. D)*. 1997. 42(2): 315-321
- Xu Z Y and Lin G. Phanerozoic tectonic evolution and its influence on the petroleum system in the middle Yangtze region. *Geotectonica et Metallogenia*. 2001. 25(1): 1-8 (in Chinese)
- Yang Z H, Zhang C L, Zhu L H, et al. The type and stage of basin-mountain transformation in continental orogeny—Taking Qinling as an example. *Earth Science Frontiers*. 1999. 6(4): 273-281 (in Chinese)
- Zhang S Y, Hao J J and Jiang T R. *A New Method to Identify the Natural Gas Type Using Carbon Isotope of the Methane and Ethane*. Beijing: Geology Press. 1988 (in Chinese)
- Zhang Y G, Zhang F K and Zhen C Y. *The Methods to Identify the Carbon Isotope*. Beijing: Geology Press. 1987 (in Chinese)
- Zhao M J, Zeng F G, Qin S F, et al. Two pyrolytic gases found and proved in Talimu Basin. *Natural Gas Industry*. 2001. 21(1): 35-38 (in Chinese)
- Zhu G Y, Zhang S C, Liang Y B, et al. The characteristics of natural gas in Sichuan Basin and its sources. *Earth Science Frontiers*. 2006. 13(2): 234-248 (in Chinese)

(Edited by Hao Jie)